Exploration of spatio-temporal correlation between AOD and precipitation rates in the Aral Sea Basin based on partial correlations

Seminar on Climate Change and Precipitation

Faculty of Geography, University of Marburg

Sarah Brüning

xxxxxxx

Darius A. Görgen

xxxxxxx

Lecturer

Dr. Boris Thies

Date

April 30, 2020

Number of words

3876

Contents

List of Figures

1 Introduction

In the last years, an increasing scientific interest has been awoken in terms of the interaction between aerosols and the elements of the hydrological cycle (Ng et al., 2017, p. 1). Precipitation patterns and their influence on human's living environment can be connected with a variety of ecological, economic and social challenges on different spatial extents (Boucher et al., 2013, p. 573 ff.). Where water is an already scarce resource, further decreases will promote rising vulnerability to external threats (Issanova et al., 2015, p. 3213ff.). In this regard, the Aral Sea region can be seen as a first-class example for investigations between aerosols and rainfall activities (Shen et al., 2019, p. 1). Deserts contain a high proportion of mineral aerosols, which may initiate climatological mechanisms of high complexity and, ultimately, a shift in precipitation rates (Boucher et al., 2013, p. 573 ff.). Still, it is hard to quantify their effects on other environmental parameters (Ng et al., 2017, p. 1). The relationship between aerosols and cloud microphysics as well as precipitation patterns remains one of the biggest uncertainties in climate studies (Altaratz et al., 2013, p. 1).

Aerosols play a major role in changes of the earth's energy budget (Ng et al., 2017, p. 1) and can be seen as an important component of global climate (Carrico et al., 2003, p. 1). There exist four major terrestrial sources for atmospheric aerosols which either absorb or scatter incoming solar and terrestrial radiation (Sharif et al., 2015, p. 657f). These direct effects may cool the surface and affect evaporation (Ng et al., 2017, p. 1). Also, aerosols act as cloud condensation nuclei (CCN) leading to more and smaller droplets which is called the first indirect aerosol effect (Costantino and Bréon, 2010, p. 1). The result is a suppression of precipitation, while the second indirect effect prolongs the cloud's lifetime through the prevention of coalescence favouring the occurrence of extreme events (Ng et al., 2017, p. 2). By heating the cloud, the coverage area is reduced, attenuating surface evaporation and further decreasing rainfall (ibid.). A number of studies showed the presence of a strong seasonality in regard to aerosol concentration in Central Asia (Ge et al., 2016, p. 62ff.; Li and Sokolik, 2018, p. 2ff.). The highest values occur in spring while the lowest concentrations have been measured in winter thus, leading to a temporal variation of aerosol effects on rainfall rates (ibid.). Some studies suggest the indicated perturbation of the hydrological cycle to be more distinct in some places than in others (Ng et al., 2017, p. 2).

Therefore, the goal of this study is to analyse temporal and spatial variations of aerosols in the Aral Sea region in relation to precipitation patterns. Following a prior seminar work regarding the analysis of aerosol and cloud microphysical properties, it continues striving for an adequate estimation of the relationship between hydro-climatological parameters. The analysis consists of the investigation of potential trends, their strength and direction in regard to aerosol concentration to rainfall rates. In order to display the overall effects, cloud microphysical parameters will be included as well as the atmosphere's relative humidity because of its critical role on rainfall variability (Altaratz et al., 2013, p. 1f.; Carrico et al., 2003, p. 2). Some studies suggest high rain rates to be associated with a rising aerosol concentration (Boucher et al., 2013, p. 4). Otherwise, contrary results have been observed as well (Ng et al., 2017, p. 1ff.). In general, time and space seem to be crucial (Grandey et al., 2014, p. 5678ff.). The hygroscopicity of aerosols causes the relative humidity to be one of the most important drivers for the observed relationship between AOD and rainfall (Ng et al., 2017, p. 2f.). When it reaches a certain concentration, it can alter the results of correlation analyses mainly through two effects (Altaratz et al., 2013, p. 1f.). First, relative humidity may cause substantial growth of the particles in an humid environment (Carrico et al., 2003, p. 1), leading to coalescence of the droplets (Ng et al., 2017, p. 2ff.). This depicts a rather positive relation between the variables (Grandey et al., 2014, p. 5678). Second, wet scavenging of aerosols through rainfall occurs in a mostly convective environment (Grandey et al., 2014, p. 5680ff.). It acts as an aerosol sink and results in a negative relationship between the aerosol concentration and precipitation or rather relative humidity (ibid.). Consequently, a negative correlation may not only reflect suppressed precipitation but also the effect mentioned above (Ng et al., 2017, p. 9). Both effects demonstrate the importance of the atmospheres' humidity in questions of aerosol-precipitation relationships and thus will be evaluated in the following study.

2 Data and Methods

2.1 Study area

The Aral Sea basin is located in the border region between Kazakhstan and Uzbekistan (57 – 67 °E, 42 – 49 °N) and acts as the tail-end lake of the contributing rivers Amu Darya and Syr Darya (Fig. 1). The study area is part of the global dust belt and shows typical features of a temperate continental climate with semi-arid to arid conditions. The summers are short and hot with a mean of 28.2 $°C$ while winters are long and cold with a mean of -3.6 $°C$. Precipitation rates are quite low with a mean of about 82.1 $mm/year$ and a maximum during winter (Gaybullaev et al., 2012, p. 287). The Aral Sea once has been the fourth largest lake on earth covering a water volume of 1.093 km^3 in 1960 (Gaybullaev et al., 2012, p. 286). Since then, it has been gradually shrinking due to over-exploitation of its natural resources by water abstraction for irrigation agriculture as well as the impacts of climate change (Ge et al., 2016, p. 2; Shen et al., 2019, p. 2031). In the year 2003, it finally split into eastern and western parts. The exposed lake bed consists of salt soils and loose sand dunes turning the former southern and western part of the lake into the Aralkum desert (Shen et al., 2019, p. 2031f., 2016, p. 624) which comprises of 57.500 km^2 (Opp et al., 2019, p. 3). The landscape is characterized by frequent salt and sand dust storms which may bear several threats to the ecosystem and local human's health (Ge et al., 2016, p. 4). It has been stated that the spatial and temporal dust deposition variability is highly significant (Opp et al., 2019, p. 1ff.).

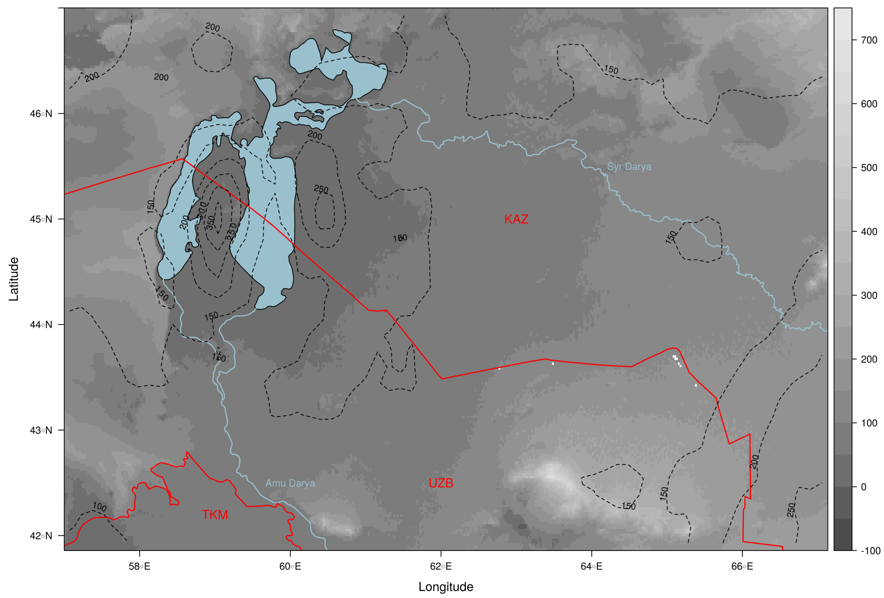

Figure 1: Overview of the study domain within the ASB (Grey-scale values represent elevation, solid red lines national boundaries and dashed isolines average yearly sums of precipitation based on CHIRPS for the years 2003-2018).

2.2 Satellite products

The aerosol and cloud properties were retrieved from the corresponding MODIS (Moderate Resolution Imaging Spectroradiometer) products MOD/MYD04 and MOD/MYD06. An explanation of the retrival processes are found in our previous seminar work.

2.2.1 Precipitation

Precipitation (P): Monthly sums of precipitation are derived from the CHIRPS data set. This data set is established by taking long-term monthly average data from ground stations in conjunction with observations from five satellite missions to establish a local regression model with a moving window for each grid cell of 0.05 ° in size (Funk et al., 2015, p. 3f.). Potential residuals in comparison to the FAO climate normals are interpolated using inverse distance weighting and are than added to the local estimates (Funk et al., 2015, p.

3). In a last step, for every pixel the five nearest ground stations are used to apply another inverse distance weighting algorithm. Here, an estimate of the decor-relation slope from the predicted precipitation and the observed precipitation at the neighboring stations are used to calculated a weighted average (Funk et al., 2015, p. 3).

2.2.2 Relative Humidity

Relative Humidity (RH): RH is retrieved using the ERA-5 reanalysis data set processed by the European Centre for Medium-Range Weather Forecasts (ECMWF) (Forecasts, 2017). This data set combines observations and model predictions to get a comprehensive model of global atmospheric conditions at small time steps and a nominal resolution of 31 km at the ground, however the data has been regridded to 0.25 °. Here, we used the monthly aggregates of RH only for the first seven atmospheric layers (1000 hPa - 850 hPa) since they were considered to represent an appropriate height level, because local aerosol transports in the region are merely reported to be found above 5 km in height (Chen et al., 2013, p. 14ff.).

2.3 Methodology

AOD and the cloud parameters were extracted from the respective MODIS data sets using the HEG-Tool (HDF-EOS To GeoTIFF Conversion Tool). More specific working steps are described in our previous seminar work, however, we aggregated all data sets to the nominal resoultion of AOD which is 10 x 10 km. Individual observations were first aggregated to a monthly temporal-resolution. From there, average values were calculated for four different seasons (Spring: March, April, May (MAM); Summer: June, July, August (JJA); Autumn: September, October, November (SON); Winter: December, January, February (DJJ)) for every year between 2003 to 2018.

The CHIRPS data set already represents monthly aggregates. The cell values were resampled to the 10 km resolution of the MODIS data and seasonal aggregates were calculated as described above. For RH, the process was basically identical, except that the median was calculated across the seven vertical layers, before the data was resampled to the same resolution as the other data sets.

To retrieve the correlation between AOD and P and to generate insights to the underlying processes we conduct a number of correlation analysis between these two parameters, while eliminating the influence of cloud parameters and RH. For this approach, we firstly checked if the data fulfills the assumptions to calculate Pearson's correlation. All variables are continuous in form. Pearson's correlation additionally is sensitive for outliers. Similarly to other studies we thus excluded exceptional high AOD values above

0.3. We then calculated the correlation coefficient between AOD and P while controlling for any other variable. This is achieved by calculating the partial correlation which is used as a measure of the linear dependence between two variables while controlling for the influences of a third. In fact, not the original values of AOD and P are fitted, but rather the residuals which were calculated by using the control variable as a predictor. Thus, only the proportion of variance which cannot be explained by the control variable is subject to the correlation analysis (Salkind, 2010). This approach has been chosen by a number of recent studies investigating relationships between aerosols and cloud microphysics as well as precipitations and seems reasonable to achieve both, investigating the "true" relationship between AOD and P in a complex field of intervening processes and effects and to deliver indications for the dominant processes driving this relationship (Engström and Ekman, 2010; Gryspeerdt et al., 2014; Ng et al., 2017).

The results of this analysis are presented on a pixel basis for each season to display spatial and temporal differences. Additionally, the correlation of all pixels which show a significant relationship at the 95 % confidence interval is calculated to investigate the overall direction and strength of correlation between aerosol and cloud parameters (Alam et al., 2010, p. 1170f.).

3 Results

3.1 Temporal and spatial variations of P and RH

The temporal and spatial variations of several aerosol and cloud parameters have been presented in the previous seminar paper. Here, we only represent the additional parameters P and RH.

Temporal and spatial dynamics for P: During the time series under study (2003 - 2018) we can observe a varying pattern for precipitation (Fig. 2). In 2003 we observe relatively high precipitation rates with an average above 200 mm per pixel and a median even slightly higher than the mean, which is in accordance with another study reporting 2003 as a very-wet year in Central Asia (Xu et al., 2016, p. 394). This amount of high precipitation rates is not reached again, instead most of the years indicate a mean value of precipitation below 150 mm per pixel. The years 2008, 2011, and 2014 show exceptional low precipitation, which are not completely in line with the findings of Xu et al. (2016). In 2015 and 2016 precipitation is higher than during the other years, however the high precipitation rate of 2003 is not reached.

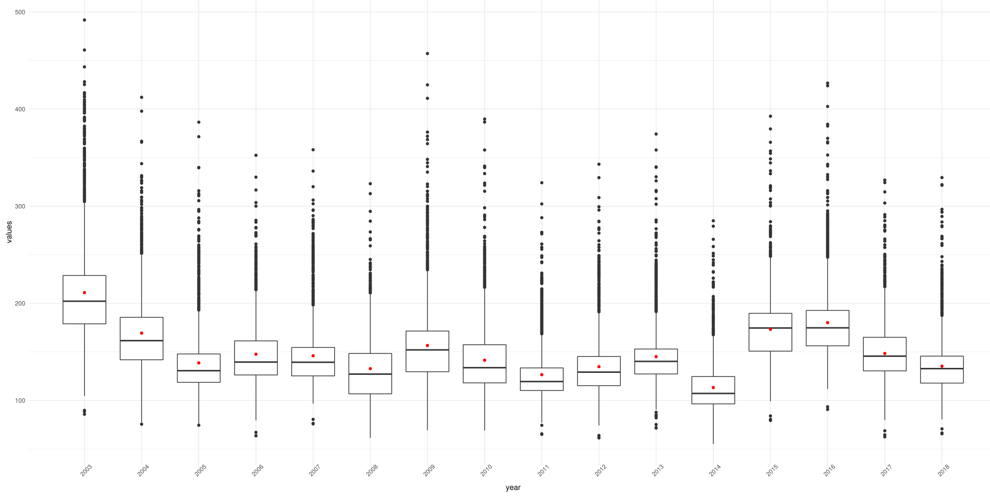

Figure 2: Boxplots for yearly sum of precipitation [mm].

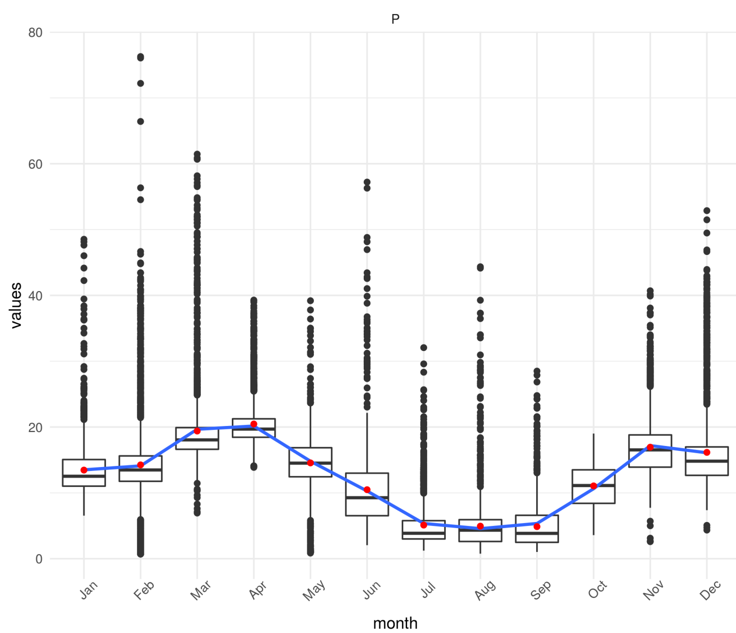

Figure 3: Boxplots for monthly sums of precipitation [mm].

Concerning the intra-annual pattern of precipitation, we observe the highest rates in March and April as well as another peak during November and December of about 19 mm per pixel (Fig. 3). During the summer months of July to September we observe the lowest precipitation rates with means about 5 mm. The seasonality of precipitation is clearly visible, with very dry conditions from June to September and relatively wet conditions from October to May.

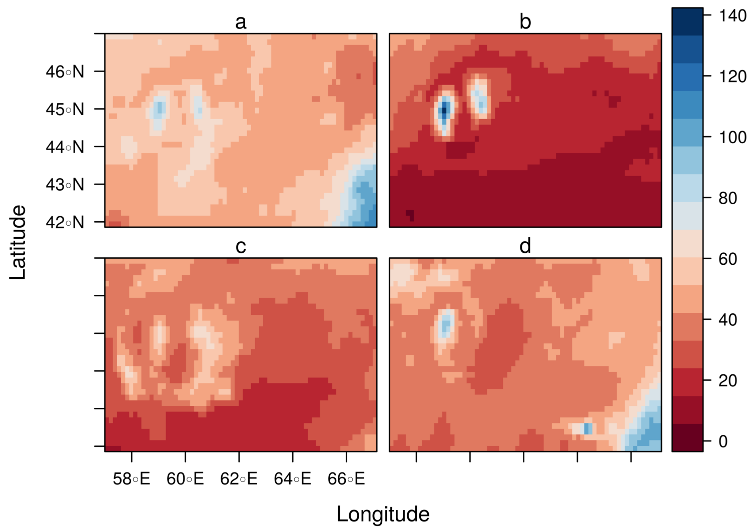

Figure 4: Spatial distribution of seasonal means for P for MAM (a), JJA (b), SON (c), and DJF (d).

The spatial pattern of P shows that higher precipitation rates are found North of the Aral Sea and Aralkum desert (Fig. 4) as well as in the South-East of the study area during the first and fourth season. The second and third season are characterized by very low precipitation rates, especially in the South of the study area. The linear trend analysis indicates significant linear trends only during the first season in the South-East of the study area. Here, moderate to high negative slopes seem to dominate the trend (about -2 to -5 mm/year). During the second season we also observe a moderate to high decrease of precipitation rate close to the Aral Sea and its Northern neighborhood. During the third and fourth season we barely observe patterns of significant linear trends.

Temporal and spatial dynamics for RH: Concerning the inter-annual dynamic of relative humidity, we observe a general decrease of RH per pixel during the first few years (Fig. 5). Similar to P, the highest level of RH is reached in 2003 with a mean value of 50%. In 2010 and 2014, we observe RH values below 40 %, and in 2012 and 2018 RH reaches only about 42 %. With the exception of 2014, we do not see the gravity of the drought years of 2008 and 2011 in the dynamic of RH. During most other years RH usually reaches between 43 - 46 %. In 2015 and 2016 the mean is about 48 %, which are the same years we observed relatively high precipitation rates.

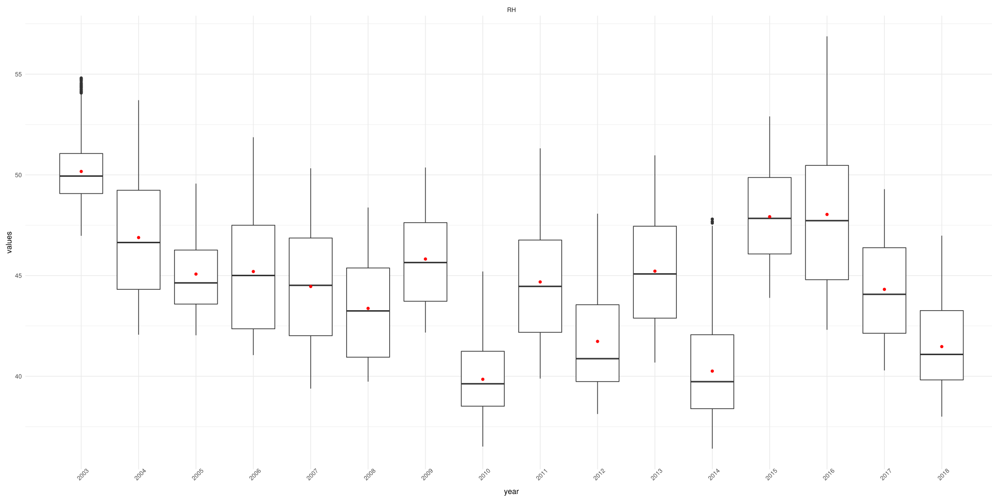

Figure 5: Boxplots for yearly median of relative humididty [%].

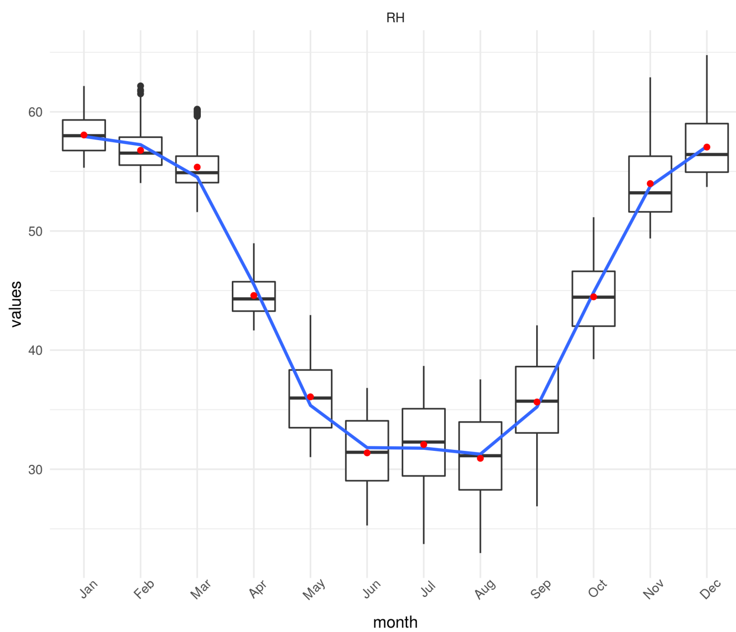

Figure 6: Boxplots for monthly median relative humidity [%].

The intra-annual dynamic of RH follows a very clear seasonal pattern with the lowest RH (~31 %) found in the warm summer months June to August (Fig. 6). RH is maximized during December to March, with levels between 55 - 58 %. The spatial pattern of RH shows higher values through the study area for the first and fourth season (Fig. 7). For the second and fourth season, the pattern is very similar with the lowest RH found in the South-East and a positive gradient towards the North-West of the study area. However, the values during the second season are substantially lower than compared to the third. Significant linear trends are only found during the second season South of the Aral Sea. Here, low negative slopes dominate the trend (about -0.3 %/year).

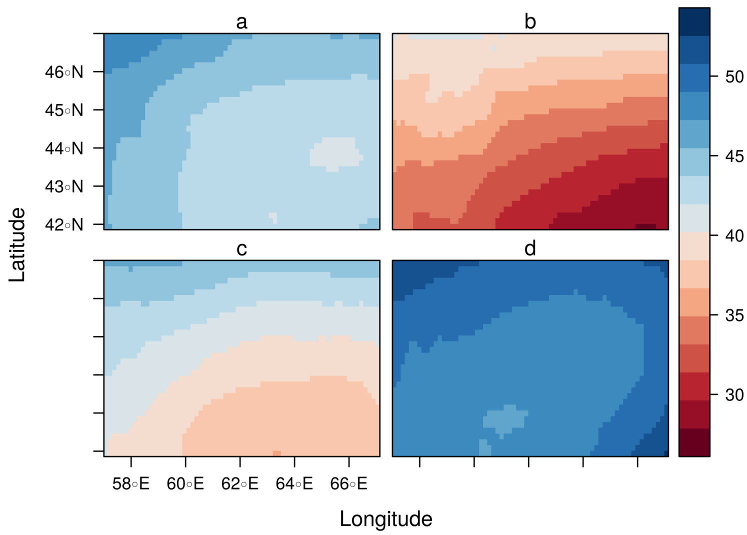

Figure 7: Spatial distribution of seasonal means for RH for MAM (a), JJA (b), SON (c), and DJF (d).

3.2 Correlation analysis between AOD and P

As indicated in the methods section, we analysed the partial correlation between AOD and P controlling for three parameters of cloud microphysics and RH. As a baseline we also calculated the correlation without any controlling variable. We excluded all pixels for which there were no observations in AOD at any time step in order to capture the complete time series of the remaining pixels. These areas are indicated in grey color in the figures below.

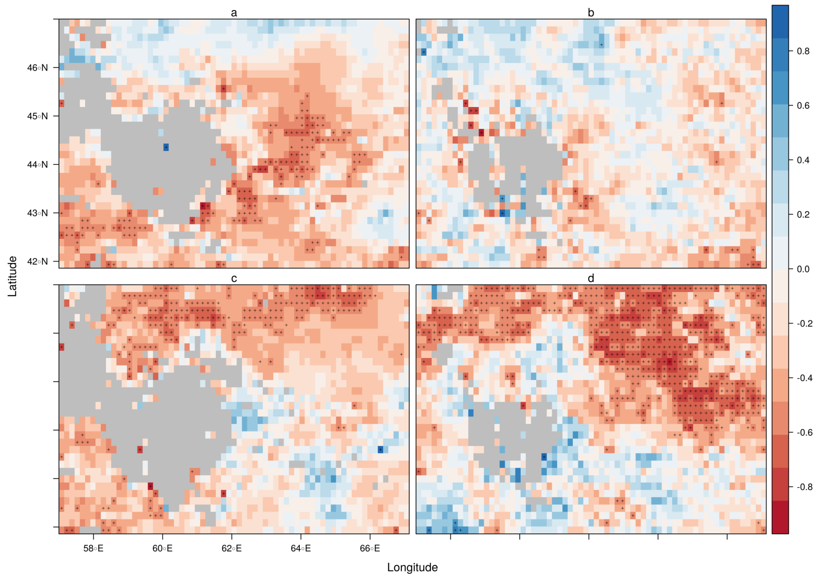

Figure 8: Spatial distribution of correlation coefficient rho between AOD and P for MAM (a), JJA (b), SON (c), and DJF (d).

Baseline correlation: Areas with missing values are concentrated around the Aral Sea in all seasons (Fig. 8). During the first and third season, the number of missing observations is higher than during the other seasons. For the first season, we observe a pattern of strongly negative correlations in the centre of the study area and South of the Aral Sea. We also observe some, though non-significant, positive correlations in the North and the far South-East of the study area. During the second season, there are only very few locations with significant correlations. In general, the picture is very patchy with positive and negative correlations distributed fairly random in the study area. In the third season we observe a comprehensive patch of negative correlations in the North of the study area and positive correlations in the South. However, the positive correlations are not significant. A similar pattern, though larger in size extending to the South, is observed during the fourth season. These correlations are significant and negative and generally between -0.4 and -0.7.

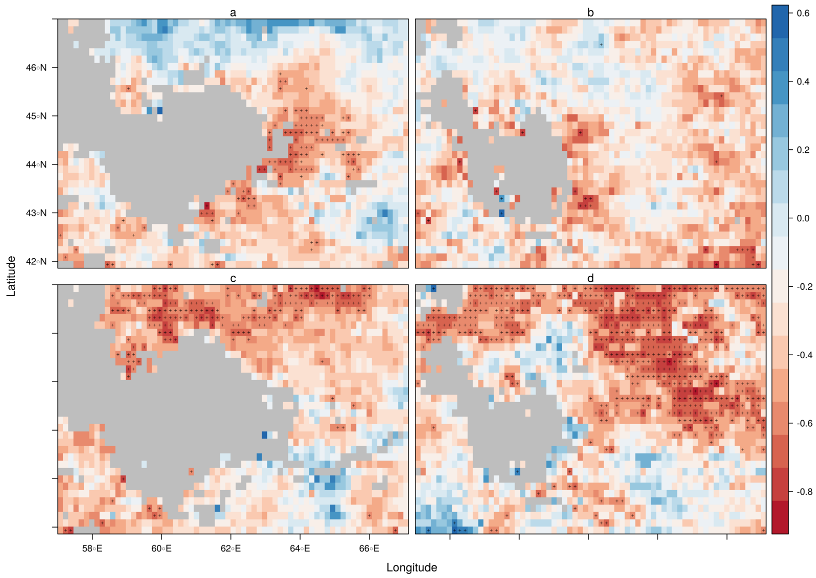

Figure 9: Spatial distribution of correlation coefficient rho between AOD and P controlled for CER for MAM (a), JJA (b), SON (c), and DJF (d).

Partial Correlation controlling for CER

Concerning the spatial distribution of the correlations, the pattern is very similar to the baseline correlation analysis (Fig. 9). However, we observe slight increases in the amplitude of the significant negative correlations for the seasons (between -0.6 and -0.85).

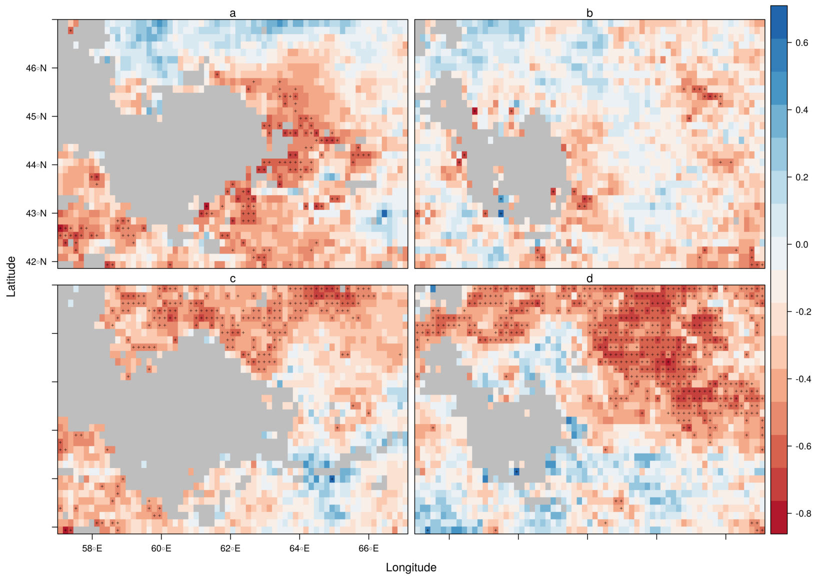

Figure 10: Spatial distribution of correlation coefficient rho between AOD and P controlled for COT for MAM (a), JJA (b), SON (c), and DJF (d).

Partial Correlation controlling for COT: The amplitude and spatial distribution is very similar to the preceding correlation analysis (Fig. 10). However, for the third and fourth season the total number of significant correlations decreases and the comprehensive areas of negative correlations are observed to become more patchy.

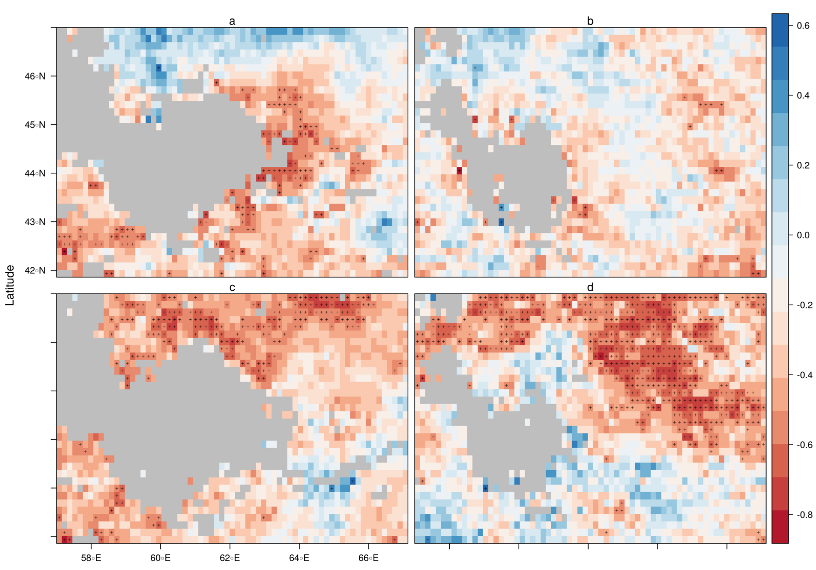

Figure 11: Spatial distribution of correlation coefficient rho between AOD and P controlled for CWP for MAM (a), JJA (b), SON (c), and DJF (d).

Partial Correlation controlling for CWP: For CWP again, the main patterns compared to the other analysis do not change (Fig. 11). However, there seems to be a slight increase in the negative correlations during the fourth season.

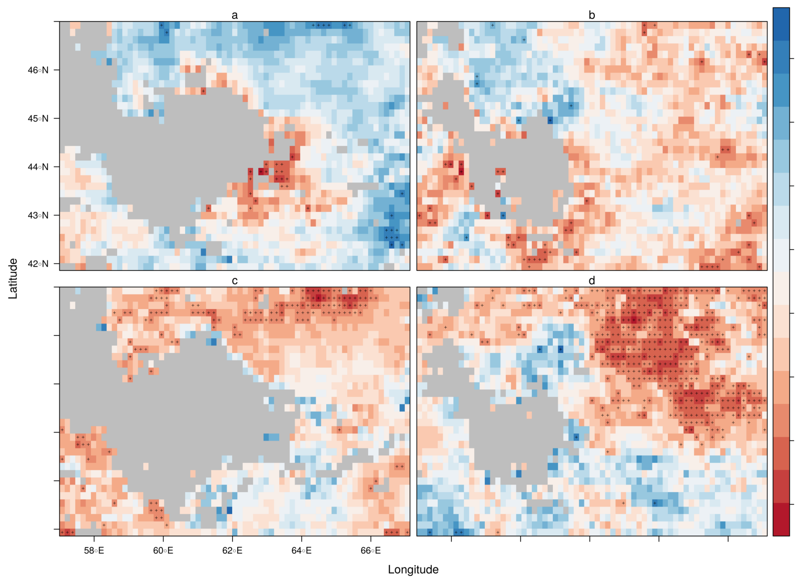

Figure 12: Spatial distribution of correlation coefficient rho between AOD and P controlled for RH for MAM (a), JJA (b), SON (c), and DJF (d).

Partial Correlation controlling for RH: When controlling for RH, some changes can be observed (Fig. 12). In the first season, the size of the patch of significant negative correlations around the Aral Sea and Aralkum desert is substantially reduced. The same finding holds true for the Norther patch of negative correlations in the third season. In the fourth season, directly North of the Aral Sea, we observe fewer significant negative correlations, however, the comprehensive patch in the centre of the study area can still be observed. In general, when controlling for RH, there seems to be a shift into the direction of positive correlations without reaching the level of significance.

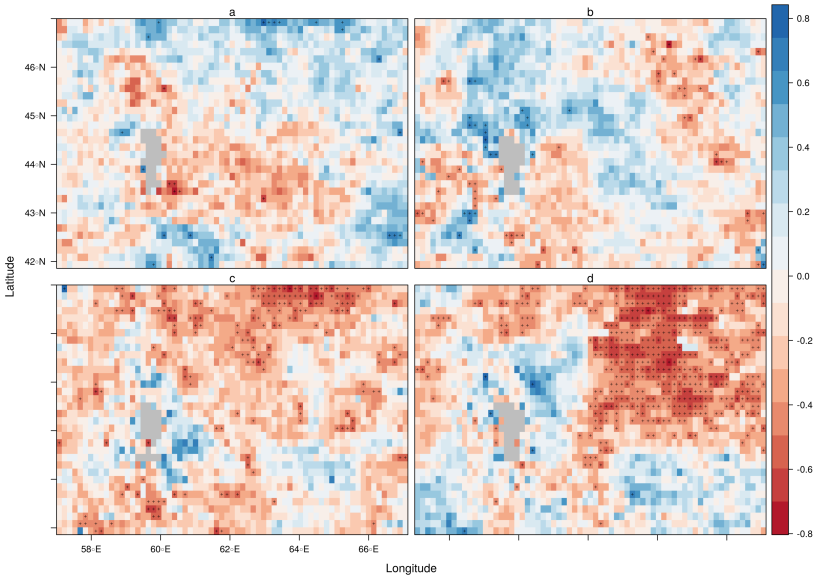

Figure 13: Spatial distribution of correlation coefficient rho between AOD and P controlled for all other variables for MAM (a), JJA (b), SON (c), and DJF (d).

Partial Correlation controlling for CWP, COT, CWP, and RH: When controlling for all variables we observe in large proportions of the study area non-significant positive and negative correlations in fairly random patterns next to each other (Fig. 13). The exceptions are a comprehensive patch of negative correlations in the North of the study area in the third season, though its size is substantially reduced compared to the baseline analysis, as well as the comprehensive patch of negative correlations in the centre of the study area during the fourth season. Compared to the analysis controlling for RH only, the non-significant positive correlations also seem to decrease in amplitude.

Analysis of significant correlations: Figure 14 shows the correlations of these selected pixels which indicated a significant correlation on the 95 % confidence intervall. The figure is divided by season and based on the controlling scenario. For all seasons and analysis we observe negative correlations between AOD and P between -0.1 and -0.38. The correlation values for the second season are substantially closer to 0 than compared to all other seasons. For the first and third season, controlling for parameters of cloud microphysics seems to increase the negative correlations compared to the baseline analysis while controlling for RH delivers smaller correlations values. For the fourth season, when controlling for RH, we observe an increase of the correlation coefficient. Controlling for cloud microphysics shows little to no effects. When all variables are controlled for, we observe no effects on the correlation coefficient for the first and fourth season. In the third season, controlling for all variables decreases the coefficient from -0.38 to -0.28.

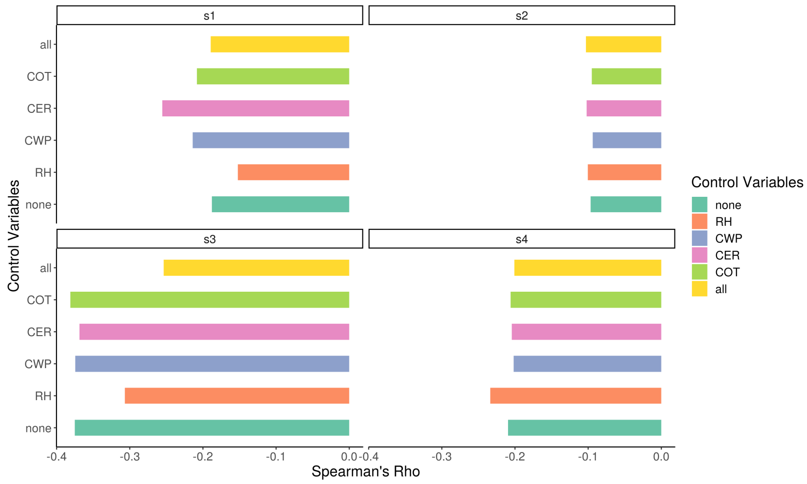

Figure 14: Correlation coefficients for all pixels with significant correlations by season.

4 Discussion

The results show the absence of a linear trend for the precipitation rates and the relative humidity. Otherwise, a distinct seasonal pattern which is coinciding between both parameters can be assumed. This depicts a high spatial variability with a confirmation of the assumptions made before concerning the hydrological cycle for Central Asia (Li and Sokolik, 2018, p. 2f.).

Beyond that, the relationship between AOD and precipitation controlled for cloud microphysical parameters as well as the relative humidity was analysed. Depending on the seasons, the correlation analyses imply the existence of diverging effects. Over all seasons, primary negative correlations turn out to be significant with a medium to high strength. In general, this contradicts the hypotheses of hygroscopic growth in the region which would lead to a strong positive relationship (Ng et al., 2017, p. 10ff.). Instead, other effects seem to dominate the existing relationship. In spring, low AOD values correlate with high precipitation rates. When using the cloud microphysics as a control variable, this pattern is not changed. Contrary, building the partial correlation with RH inverts the direction of the correlation. This corresponds with other studies' findings about a wet scavenging effect in Central Asia during wet seasons (Grandey et al., 2014, p. 5682f.).

In summer, the very low precipitation rates (<5 mm) prevent the formation of distinct effects between aerosols and rainfall rates. As a result, only scattered patches of correlations occur. In autumn, the dry conditions attenuate the precipitation rates in September, thus influencing the outcome of the correlation analysis. In the north of the study area, negative correlations appear. The partial correlation analysis reveals that RH is not the primary driver. Also, a direct influence of the depicted cloud microphysics cannot be assumed. Instead, the effects may originate from unknown effects, like meteorological parameters or satellite retrieval biases (Ng et al., 2017, p. 11.). During winter, a similarly strong patch of negative correlations is visible in the northern parts of the study area, which prevails when controlling for other parameters. This finding impliesnone of the investigated parameters dominates the correlation analysis. Only a small portion around the northern edge of the Aral Sea pictures RH to be a primary driver. The analysis indicates a highly temporal variety of effects between the seasons as well as spatial diverse formations within the study area. Depending on spatio-temporal conditions the relationship between aerosol concentration and precipitation patterns is driven by different parameters. In months with a high moisture, relating effects arise (Altaratz et al., 2013, p. 4f.). Wet scavenging as described by Grandey et al. (2014) may play a major role in parts of the study area and can form an aerosol sink, leading to positive correlations when it is accounted for RH. In contrast, the characteristics of the aerosols may suppress hygroscopic growth, leading to negative correlations.

In regards to the aerosol type, these effects could be attributed to the dominance of mineral aerosols, but an comprehensive analysis is not feasible with the data at hand (Altaratz et al., 2013, p. 4f.). Dry conditions promote ambiguous effects which cannot be traced back to the investigated parameters alone. However, RH seems to be one of the main drivers of the aerosol-rainfall relationship. Accounting for RH, reveals rather positive correlations between AOD and precipitation in wet conditions during spring, while the contrary is observed during winter. Thus, the relationship between aerosol and precipitation data implies in parts a rainfall suppression, but these findings are not adequately pictured in the correlation to cloud properties (the reader is referred to our previous seminar work). It remains unknown whether indirect aerosol effects like the suppression of precipitation in context to the Twomey- or Albrecht-effect occur in the study area. As a result, the study's hypotheses can be neither confirmed not denied. Instead, a more detailed analysis would provide deeper insights into ongoing processes not just for the aerosol-cloud interactions but also for the relationship to the precipitation patterns (Ng et al., 2017, p. 11f.). First, the choice of seasons is not ideal for the study area due to a big inter-annual variance in moisture. Regardless of the division, months with relatively high and low values may be sampled within the same seasons. Second, an additional source of error may be the existence of a large-scale meteorological variability (Altaratz et al., 2013, p. 4f.). Especially in data sparse regions, a higher resolution for observing meteorological parameters could enhance the knowledge of the ongoing processes. In the context of satellite retrieval bias, failed data acquisition or data inhomogeneity, further evaluation is necessary (Grandey et al., 2014, p. 5683). Nonetheless, first results for the hydrological cycle can be derived. Wet-scavenging as well as interactions of aerosols with cloud microphysics can lead to changes in the relationship between aerosols and precipitation. However, the effects vary in time and space, leading to either precipitation enhancement or suppression. Tracking of the aerosols' origin in addition to an analysis of the vertical structure and aerosol type can ensure more reliable results (Sharif et al., 2015, p. 660ff.).

5 Conclusion

The subsequent analysis of hydrological connectivity to the aerosol characteristics enhances the demand for further investigations in this field of interest. An adequate quantification of ongoing processes is even more complex than it was thought to be, resulting from technological issues as well as natural mechanisms which tend to overlay each other and promote distortion of each other's effects. Thus, answering the question of the strength and direction of relationship between aerosol and precipitation properties is aggravated. The study implies the existence of moisture related processes like wet scavenging but also the suppression of drizzle due to aerosol-cloud interactions. Therefore, only a temporal and spatial approximation of effects in the Aral Sea region can be gathered from the data. Further research in this highly vulnerable environment is crucial for assessing the situation with reliable insights.

6 References

Alam, K., Iqbal, M.J., Blaschke, T., Qureshi, S., Khan, G., 2010. Monitoring spatio-temporal variations in aerosols and aerosol-cloud interactions over Pakistan using MODIS data. Advances in Space Research 46, 1162–1176. https://doi.org/10.1016/j.asr.2010.06.025

Altaratz, O., Bar-Or, R.Z., Wollner, U., Koren, I., 2013. Relative humidity and its effect on aerosol optical depth in the vicinity of convective clouds. Environmental Research Letters 8. https://doi.org/10.1088/1748-9326/8/3/034025

Boucher, O., Randall, D., Artaxo, P., Bretherton, C., Feingold, G., Forster, P., Kerminen, V.-M., Kondo, Y., Liao, H., Lohmann, U., Rasch, P., Satheesh, S., Sherwood, S., Stevens, B., Zhang, X., 2013. Clouds and Aerosols, in: Stocker, T., Qin, D., Plattner, G.-K., Tignor, M., Allen, S., Boschung, J., Nauels, A., Xia, Y., Bex, V., Midgley, P. (Eds.), Climate Change 2013: The Physical Science Basis. Contribution of Working Group I to the Fifth Assessment Report of the Intergovernmental Panel on Climate Change. Cambridge University Press, Cambridge, United Kingdom; New York, NY, USA., pp. 465–657. https://doi.org/10.1017/CBO9781107415324.015

Carrico, C.M., Kus, P., Rood, M.J., Quinn, P.K., Bates, T.S., 2003. Mixtures of pollution, dust, sea salt, and volcanic aerosol during ACE-Asia: Radiative properties as a function of relative humidity. Journal of Geophysical Research D: Atmospheres 108. https://doi.org/10.1029/2003jd003405

Chen, B.B., Sverdlik, L.G., Imashev, S.A., Solomon, P.A., Lantz, J., Schauer, J.J., Shafer, M.M., Artamonova, M.S., Carmichael, G.R., 2013. Lidar Measurements of the Vertical Distribution of Aerosol Optical and Physical Properties over Central Asia. International Journal of Atmospheric Sciences 2013, 1–17. https://doi.org/10.1155/2013/261546

Costantino, L., Bréon, F.M., 2010. Analysis of aerosol-cloud interaction from multi-sensor satellite observations. Geophysical Research Letters 37. https://doi.org/10.1029/2009GL041828

Engström, A., Ekman, A.M., 2010. Impact of meteorological factors on the correlation between aerosol optical depth and cloud fraction. Geophysical Research Letters 37, 1–4. https://doi.org/10.1029/2010GL044361

Forecasts, E.C. for M.-R.W., 2017. ERA5 Reanalysis (0.25 Degree Latitude-Longitude Grid). https://doi.org/https://doi.org/10.5065/BH6N-5N20

Funk, C., Peterson, P., Landsfeld, M., Pedreros, D., Verdin, J., Shukla, S., Husak, G., Rowland, J., Harrison, L., Hoell, A., Michaelsen, J., 2015. The climate hazards infrared precipitation with stations - A new environmental record for monitoring extremes. Scientific Data 2, 1–21. https://doi.org/10.1038/sdata.2015.66

Gaybullaev, B., Chen, S.-C., Gaybullaev, D., 2012. Changes in water volume of the Aral Sea after 1960. Applied Water Science 2, 285–291. https://doi.org/10.1007/s13201-012-0048-z

Ge, Y., Abuduwaili, J., Ma, L., Liu, D., 2016. Temporal Variability and Potential Diffusion Characteristics of Dust Aerosol Originating from the Aral Sea Basin, Central Asia. Water, Air, and Soil Pollution 227. https://doi.org/10.1007/s11270-016-2758-6

Grandey, B.S., Gururaj, A., Stier, P., Wagner, T.M., 2014. Rainfall-aerosol relationships explained by wet scavenging and humidity. Geophysical Research Letters 41, 5678–5684. https://doi.org/10.1002/2014GL060958

Gryspeerdt, E., Stier, P., Grandey, B.S., 2014. Cloud fraction mediates the aerosol optical depth-cloud top height relationship. Geophysical Research Letters 41, 3622–3627. https://doi.org/10.1002/2014GL059524

Issanova, G., Abuduwaili, J., Galayeva, O., Semenov, O., Bazarbayeva, T., 2015. Aeolian transportation of sand and dust in the Aral Sea region. International Journal of Environmental Science and Technology 12, 3213–3224. https://doi.org/10.1007/s13762-015-0753-x

Li, L., Sokolik, I.N., 2018. Analysis of dust aerosol retrievals using satellite data in Central Asia. Atmosphere 9. https://doi.org/10.3390/atmos9080288

Ng, D.H.L., Li, R., Raghavan, S.V., Liong, S.Y., 2017. Investigating the relationship between Aerosol Optical Depth and Precipitation over Southeast Asia with Relative Humidity as an influencing factor. Scientific Reports 7, 1–13. https://doi.org/10.1038/s41598-017-10858-1

Opp, C., Groll, M., Semenov, O., Vereshagina, N., Khamzina, A., 2019. Impact of the Aral Sea Syndrome - the Aralkum as a Man-Made Dust Source. E3S Web of Conferences 99, 03003. https://doi.org/10.1051/e3sconf/20199903003

Salkind, N., 2010. Encyclopedia of Research Design. https://doi.org/10.4135/9781412961288 NV - 0

Sharif, F., Alam, K., Afsar, S., 2015. Spatio-Temporal distribution of aerosol and cloud properties over Sindh using MODIS satellite data and a HYSPLIT model. Aerosol and Air Quality Research 15, 657–672. https://doi.org/10.4209/aaqr.2014.09.0200

Shen, H., Abuduwaili, J., Ma, L., Samat, A., 2019. Remote sensing-based land surface change identification and prediction in the Aral Sea bed, Central Asia. International Journal of Environmental Science and Technology 16, 2031–2046. https://doi.org/10.1007/s13762-018-1801-0

Shen, H., Abuduwaili, J., Samat, A., Ma, L., 2016. A review on the research of modern aeolian dust in Central Asia. Arabian Journal of Geosciences 9. https://doi.org/10.1007/s12517-016-2646-9

Xu, H. jie, Wang, X. ping, Zhang, X. xiao, 2016. Decreased vegetation growth in response to summer drought in Central Asia from 2000 to 2012. International Journal of Applied Earth Observation and Geoinformation 52, 390–402. https://doi.org/10.1016/j.jag.2016.07.010